Supplementary Material (ESI) for Journal of Materials Chemistry

Supporting Information

Magnetic Nanoparticles with Functional Silanes: Evolution of Well-defined Shells from Anhydride Containing Silane

Xinlei Huang[a], Abrin Schmucker[a], Jason Dyke[a], Sara M. Hall[a], John Retrum[a], Barry Stein[b], Nicholas Remmes[c], David V. Baxter[c], Bogdan Dragnea[a], Lyudmila M. Bronstein[*a]

Indiana University, Departments of Chemistry[a], Biology[b], and Physics[c], Bloomington, IN 47405, USA

[*] To whom correspondence should be addressed (lybronst@indiana.edu)

Figure S1. FC and ZFC magnetization curves of **NP1** before (a) and after (b) coating with AHAPS.

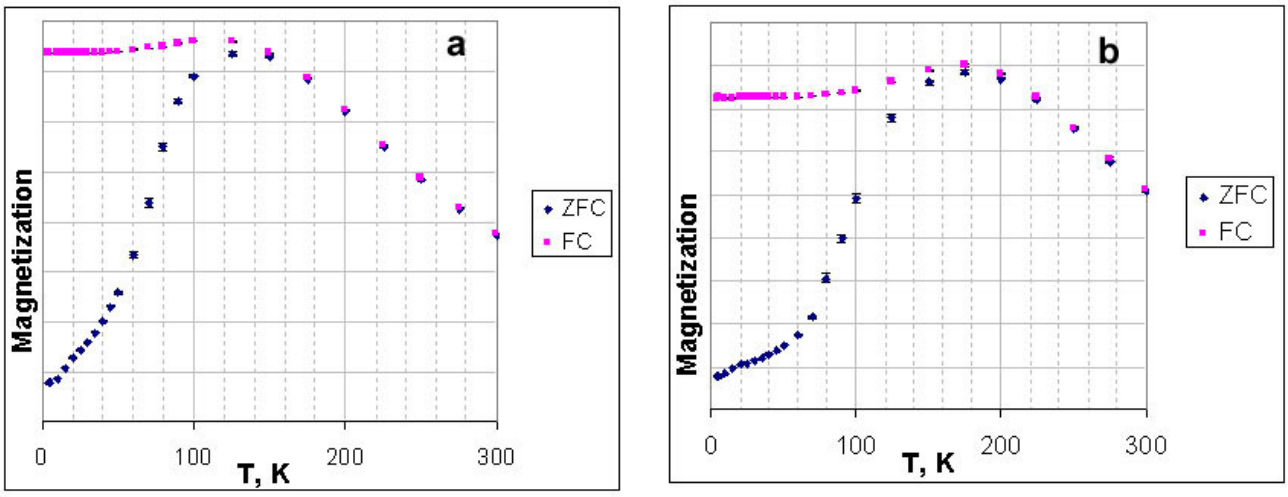

FC and ZFC curves of **NP1** before and after coating with AHAPS are presented in Figure S1, allowing us to confirm the superparamagnetic nature of the particles and to provide some additional insight on the interparticle interactions. It is noteworthy that below a temperature T_b (the blocking temperature which corresponds roughly to the peak position in the ZFC data in Figure S1) the movement of magnetic moments is blocked and their magnetization is irreversible, whereas above T_b the magnetization is reversible and the particles are superparamagnetic.[1, 2] The blocking temperature is sensitive to the particle size and anisotropy (which should not change with changes in the coating, see below) and the interparticle interactions (which could change with changes to the coating).

The blocking temperature increases from 130 to 180 K when the particles are functionalized with AHAPS, revealing the stronger interparticle interaction after AHAPS attachment. This is

consistent with the fact that AHAPS is shorter than oleic acid (~1.2 nm vs ~1.7 nm of extended length) and contains amino groups which form hydrogen bonds; both factors ensure the shorter interparticle distance.[3, 4] In the case of amino groups adsorbed on the NP surface (see discussion of FTIR spectra), the shell can be even thinner.

The room temperature (300 K) magnetization curves of **NP1** before and after coating with AHAPS are presented in Figure S2. The magnetization curves are normalized to the Fe_2O_3 content using elemental analysis data on Fe, and a correction of about 10% is made in the scaling of one of the curves so that the curves overlap (a correction within the approximate uncertainty in the mass and elemental analysis data of the measured samples). The shape of the M-H magnetization curves above the blocking temperature are highly sensitive to particle size, so the good overlap of the two curves shows that the particles are essentially identical in the two samples, revealing that no changes in the nanoparticle nature take place during functionalization. The model curve is intended as a reference and shows what the magnetization curve of monodisperse superparamagnetic particles with a moment per particle of about 4000 μ_B would look like. The rough agreement between the model and the measurements, when combined with the ZFC-FC data discussed above, indicate that the particles are almost certainly superparamagnetic with a magnetic moment per particle of a several thousand Bohr magnetons.

Figure S2. Magnetization curves of **NP1** before and after coating with AHAPS. The model shows the expected curve for monodisperse superparamagnetic particles with a moment per particle of about 4000μ_B.

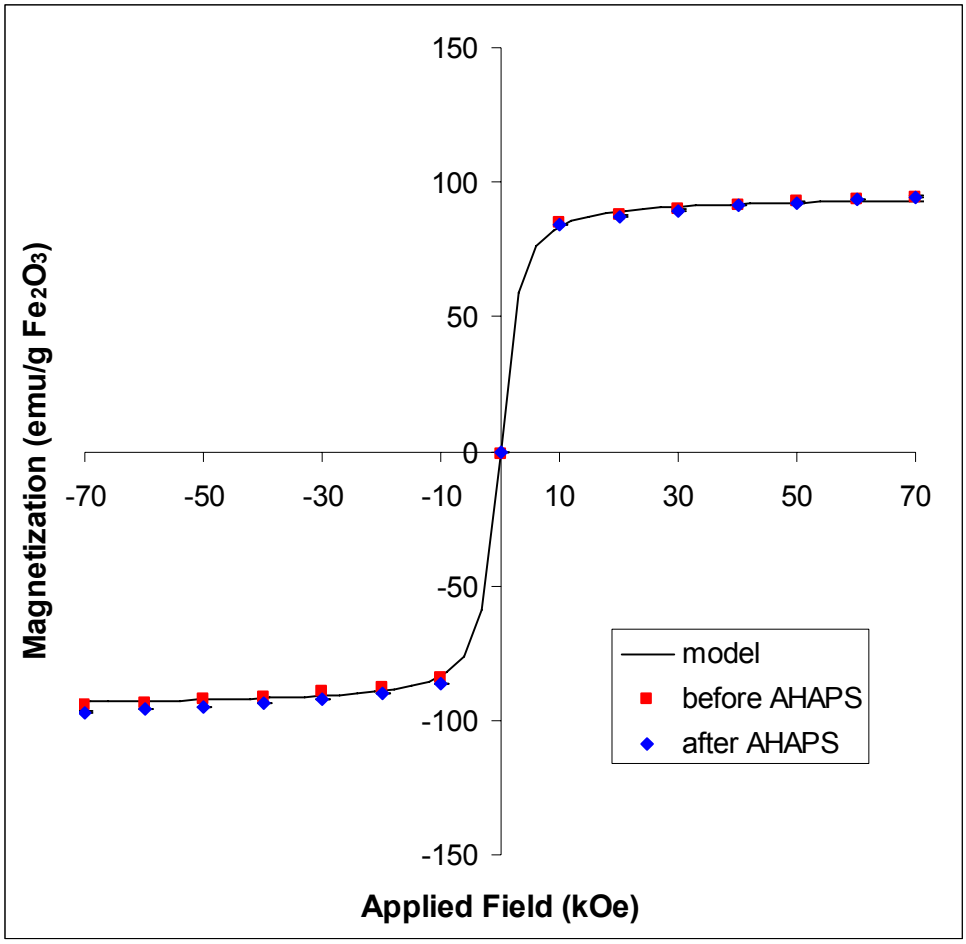

Figure S3. DLS volume distributions vs. hydrodynamic diameter for **NP1**-AHAPS, **NP2**-AHAPS, and **NP3**-AHAPS.

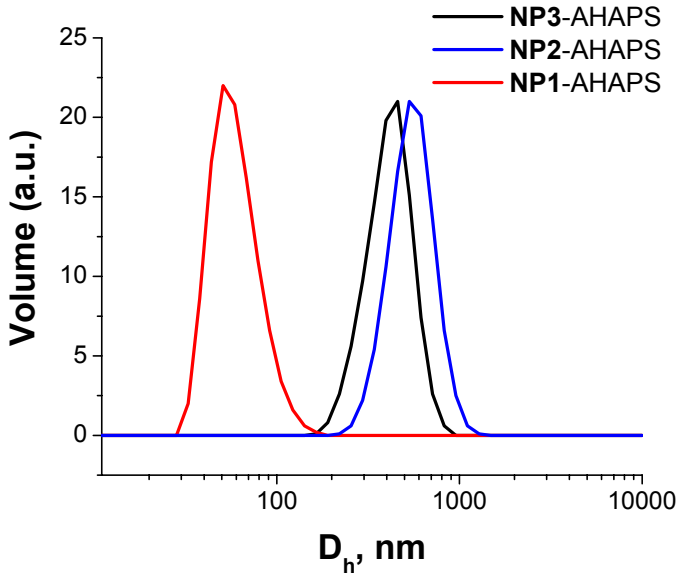

Figure S4. TEM image of **NP2**-AHAPS. The nanoparticles form stable aggregates.

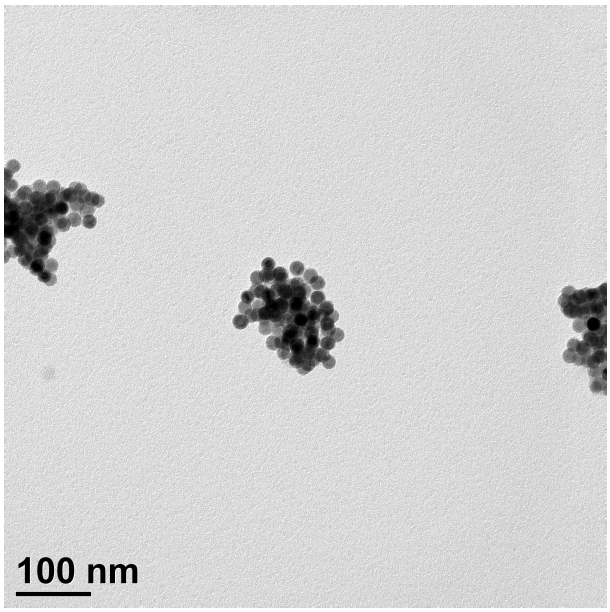

Figure S5. FTIR spectra of AHAPS, **NP2** and **NP2**-AHAPS.

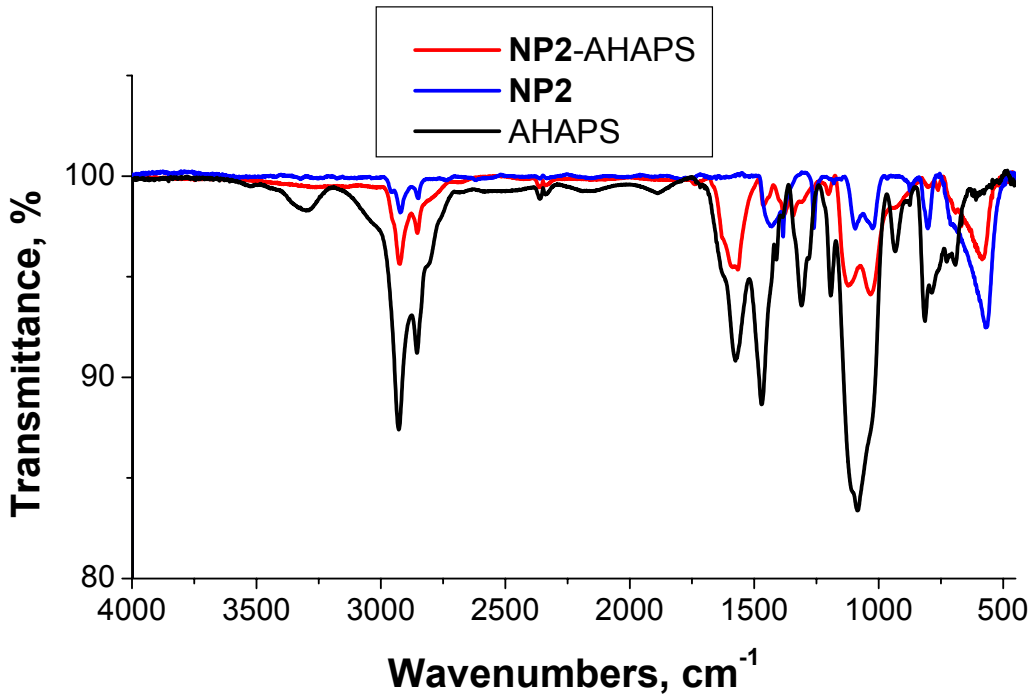

The first indication of the Fe-O-Si bond formation is a broadening and shift of the Fe-O band from 570 to 584 cm^{-1}.[5] We also observed distinct differences between the FTIR spectra of neat AHAPS and **NP2**-AHAPS. One of these differences is observed in the 1000-1100 cm^{-1} frequency region. In the FTIR spectrum of neat AHAPS this region is dominated by the band at 1086 cm^{-1} which is assigned to Si-OCH_3 group stretching vibrations.[6] In the FTIR spectrum of **NP2**-AHAPS there are two well defined bands at 1123 and 1032 cm^{-1} which can be assigned to Si-CH_2 and Si-O-Si vibrations, respectively.[6, 7] (Note that in the **NP2** FTIR spectrum there are much weaker bands in the same region due to the Fe-OH vibrations, see discussion to Fig. 3).

Formation of Si-O-Si bonds can occur due to three possible scenarios: (i) the interaction of neighboring silane molecules with each other with formation of a condensed AHAPS monolayer on the NP surface, (ii) the formation of multilayer shells on the NP surface, or (iii) the formation of the condensed silane material (polymeric AHAPS)[8]. The last case is hardly plausible, however, because polymeric AHAPS would be observed in the TEM images, but it is not. The small interparticle distances in the TEM images (Fig. 4) suggest formation of rather thin shell, probably a monolayer. Another argument to support this conclusion is a low ratio of the bands associated with Si-O-Si vibrations (normally very strong in polymeric products) to the band at 584 cm^{-1} ascribed to the iron oxide vibrations. Another significant difference between the FTIR spectra of AHAPS and **NP2**-AHAPS can be observed in the 1500-1300 cm^{-1} frequency region. The strong band in the AHAPS spectrum at 1470 cm^{-1}, associated with $CH_3(O)$ vibrations[9] is significantly decreased due to condensation and attachment to the iron oxide surface. It is noteworthy that the CH_2 deformations are also observed in this region so the band at 1462 cm^{-1} in the **NP2**-AHAPS spectrum may include both types of vibrations.[10]

Figure S6. DLS volume distributions vs. hydrodynamic diameter for NPs coated with SSA (150 min reaction time) in THF after purification of the reaction solution and in water after hydrolysis.

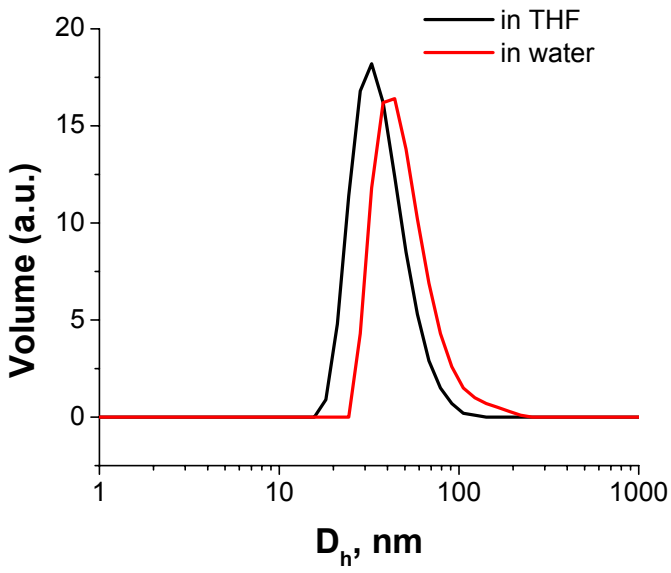

References

1. Petit, C.; Taleb, A.; Pileni, M. P. *Adv. Mater.* **1998,** 10, (3), 259.
2. Talapin, D. V.; Shevchenko, E. V.; Weller, H., Synthesis and Characterization of Magnetic Nanoparticles. In *Nanoparticles*, Schmid, G., Ed. Wiley-VCH: Weinheim, 2004; pp 199.
3. Vestal, C. R.; Song, Q.; Zhang, Z. J. *J. Phys. Chem. B* **2004,** 108, (47), 18222.
4. Dai, J.; Wang, J.-Q.; Sangregorio, C.; Fang, J.; Carpenter, E.; Tang, J. *J. Appl. Phys.* **2000,** 87, (10), 7397.
5. De Palma, R.; Peeters, S.; Van Bael, M. J.; Van den Rul, H.; Bonroy, K.; Laureyn, W.; Mullens, J.; Borghs, G.; Maes, G. *Chem. Mater.* **2007,** 19, (7), 1821.
6. Yim, H.; Kent, M. S.; Tallant, D. R.; Garcia, M. J.; Majewski, J. *Langmuir* **2005,** 21, (10), 4382.
7. Cheng, Q.; Li, C.; Pavlinek, V.; Saha, P.; Wang, H. *Appl. Surf. Sci.* **2006,** 252, (12), 4154.

8. Bronstein, L. M.; Linton, C.; Karlinsey, R.; Ashcraft, E.; Stein, B.; Svergun, D. I.; Kozin, M.; Khotina, I. A.; Spontak, R. J.; Werner-Zwanziger, U.; Zwanziger, J. W. *Langmuir* **2003,** 19, 7071.
9. Yuan, W.; van Oou, W. J. *J. Coll. Interface Sci.* **1997,** 185, (1), 197.
10. Remes, Z.; Kromka, A.; Vanecek, M.; Grinevich, A.; Hartmannova, H.; Kmoch, S. *Diamond & Related Mater.* **2007,** 16, (4-7), 671.